



Batch and dynamic biosorption of basic dyes from binary solutions by alkaline-treated cypress cone chips

M.E. Fernandez^{a,b}, G.V. Nunell^{a,b}, P.R. Bonelli^{a,b}, A.L. Cukierman^{a,b,c,*}

^a Programa de Investigación y Desarrollo de Fuentes Alternativas de Materias Primas y Energía (PINMATE), Departamento de Industrias, Facultad de Ciencias Exactas y Naturales, Universidad de Buenos Aires, Intendente Güiraldes 2620, Ciudad Universitaria, C1428BGA Buenos Aires, Argentina

^b Consejo Nacional de Investigaciones Científicas y Técnicas (CONICET), Av. Rivadavia 1917, C1033AAJ Buenos Aires, Argentina

^c Cátedra de Farmacotecnia II, Departamento de Tecnología Farmacéutica, Facultad de Farmacia y Bioquímica, Universidad de Buenos Aires, Junín 956, C1113AAD Buenos Aires, Argentina

ARTICLE INFO

Article history:

Received 26 September 2011
Received in revised form 30 November 2011
Accepted 1 December 2011
Available online 8 December 2011

Keywords:

Modified cone chips
Basic dyes
Competitive dynamic biosorption
Industrial effluents treatment

ABSTRACT

A simple alkaline pre-treatment of *Cupressus sempervirens* cone chips was performed to improve their biosorption capacity towards methylene blue and rhodamine B from aqueous solutions, in batch and continuous modes. Biosorption kinetics were determined from single and binary dyes solutions, and properly described by the pseudo-second-order rate model. Experimental single-dye equilibrium isotherms fitted the Langmuir–Freundlich model, with maximum biosorption capacities of 0.68 mmol/g for methylene blue and 0.50 mmol/g for rhodamine B. Single-dye dynamic biosorption showed that breakthrough time for methylene blue biosorption was almost four times longer than for rhodamine B and that the alkaline modification of the chips greatly improved the biosorption performance. Competitive dynamic biosorption demonstrated the preference of the modified cone chips for biosorbing methylene blue, confirmed by the exit concentration overshoots obtained in the breakthrough curves of rhodamine B.

© 2011 Elsevier Ltd. All rights reserved.

1. Introduction

Removal of dyes from industrial effluents is a major challenge connected to environmental and human health safety. Unfixed dyes from dying baths are discharged within common textile effluents. Over 7×10^5 ton and approximately 10^4 different dyes and pigments are produced annually world-wide, around 10% of which may be found in wastewaters (Rodríguez Couto, 2009).

Recalcitrant nature and non-biodegradability of dyes are characteristics derived from their complex structures and synthetic origin; they are specifically designed to resist fading upon exposure to light, water and oxidizing agents, and as such are very stable and difficult to degrade (Nigam et al., 2000). Dyes exhibit considerable structural diversity; those of basic nature have affinity towards materials with negatively charged functional groups like lignin, but very weak affinity for pure cellulose (Drnovšek et al., 2005). Among basic dyes, methylene blue (MB) and more recently, rhodamine B (RhB), have been used as probe molecules for the removal

of dyestuffs (Attia et al., 2003; Forgacs et al., 2004; Panda et al., 2009; Vilar et al., 2007).

There is a readily need to find effective low cost alternatives to expensive commercial activated carbon suitable to control increasing pollution in water. Natural materials that are available in large quantities, or certain waste products from industrial or agricultural operations, may have potential as biosorbents of different pollutants (Gupta and Suhas, 2009; Sud et al., 2008). Among these materials, agro-forest lignocellulosic residues have shown good biosorption capacities for some basic dyes (Batzias and Sidiras, 2004; Janoš et al., 2009). In particular female cones from conifer trees, that are abundant in wood processing fields have been recently applied for biosorption of dyes (Akar et al., 2008; Fernandez et al., 2010), mostly with no further treatment other than crushing and washing with water. Although this kind of biomass has shown a reasonable capacity, some more or less sophisticated pretreatment procedures have been developed, including treatments with mineral acids, bases or their salts (Janoš et al., 2009), to improve the biosorption ability of wood-derived materials towards these and others contaminants.

Furthermore, an efficient application of dye decolourization at industrial scale requires the performance of a continuous system technology and the consideration of more than one contaminant in effluents. Biosorption studies are frequently restricted to experiments in batch mode; though they are useful to elucidate

* Corresponding author at: Programa de Investigación y Desarrollo de Fuentes Alternativas de Materias Primas y Energía (PINMATE), Departamento de Industrias, Facultad de Ciencias Exactas y Naturales, Universidad de Buenos Aires, Intendente Güiraldes 2620, Ciudad Universitaria, C1428BGA Buenos Aires, Argentina. Tel.: +54 11 45763383; fax: +54 11 45763366.

E-mail address: analea@di.fcen.uba.ar (A.L. Cukierman).

biosorption capacities parameters for dye removal, they lack of applicability for real wastewater treatment systems. Small-scale continuous flow studies generally give accurate predictions for dye removal from real wastewater systems. Packed-bed columns are simple to operate, attain a high yield and can be easily scaled up (Akar and Divriklioglu, 2010). On the other hand, most studies have been focused on the improvement of biosorption performance for dyes in single systems, but there is few information regarding binary and multiple biosorption of organics available in literature (Anastasi et al., 2010; Yang et al., 2011) and especially in continuous flow.

In the present work, a simple pre-treatment procedure was used to modify the properties of cypress cone chips from *Cupressus sempervirens* previously studied by our research group (Fernandez et al., 2010), to improve even further the biosorption capacity towards two representative basic dyes (MB and RhB) from aqueous solutions, in batch and continuous modes. Kinetic and equilibrium biosorption parameters were obtained from the application of mathematical models. The interaction between the dyes in competitive studies for their biosorption on the modified material was evaluated and particular emphasis was placed on continuous removal of both dyes from single and binary solutions assessed from experiments in an up-flow column. The physicochemical and textural characteristics of the modified biosorbent were evaluated and compared with those of the untreated material.

2. Methods

2.1. Materials

C. sempervirens cypress cones were collected from Paraná River region, province of Entre Ríos in Argentina. After washing with tap water to eliminate dust and other residues, samples were dried at 60 °C and then crushed, milled and screen-sieved. The biosorbent obtained is hereafter labeled as PNAT. Fractions of particle diameter between 105 and 500 µm were selected for further chemical modification. PNAT chips were suspended in 100 mL of a 0.5 N KOH solution at a suitable ratio and the mixture was stirred using a magnetic stirrer for 60 min at room temperature. Then, it was thoroughly washed with distilled water to remove residual alkali. The product, hereafter labeled as PKOH, was again dried at 60 °C. The fraction of particle diameter between 250 and 500 µm was selected for characterization of the biosorbents and batch biosorption experiments, with the exception of kinetic assays and experiments in dynamic conditions, where samples of particle diameter between 105 and 250 µm were used.

Two basic dyes of analytical grade were used for biosorption experiments: methylene blue (basic blue 9, C.I. 52015, M.W. 373.91 g/mol) purchased from Carlo Erba®, and rhodamine B (basic violet 10, C.I. 45170, M.W. 479.02 g/mol), colorimetric reagent purchased from Sigma–Aldrich®.

2.2. Characterization of PNAT and PKOH

Proximate analysis of the cone chips samples was performed by thermogravimetric analysis (TA Instruments SDT Q600), according to American Society of Testing and Materials (ASTM) standards 5142. An automatic elemental analyzer (Carlo Erba model EA 1108) was used to assess their elemental composition.

A modified procedure based on Boehm's method (Basso et al., 2002; Fernandez et al., 2010), commonly applied for activated carbons, was used to quantify total polar/acidic oxygen functional groups (TOFG), i.e. carbonyls, phenols, lactones, and carboxyl groups, present on the biosorbent surface. Briefly, 0.5 g of the biosorbent was suspended in 50 mL of a 0.05 N solution of sodium

ethoxide and the slurries were stirred for 24 h. After filtering, an aliquot of the resulting solution was added to a volume of a 0.05 N HCl solution and subsequently back-titrated with 0.05 N NaOH. Likewise, total basic surface groups (TBG) were determined on PNAT and PKOH chips by contacting the same amount of biosorbent with 50 mL of 0.05 N HCl solutions. The slurries were also stirred for 24 h and after filtering; an aliquot of the resulting solution was titrated with a 0.05 N NaOH solution. Average values expressed as milliequivalents per gram of sample are reported.

Furthermore, identification of surface functionalities on PNAT and PKOH was complementary conducted by Fourier Transformed infrared (FT-IR) spectroscopy. The spectra were recorded using a Perkin–Elmer IR Spectrum BXII spectrometer within the range 600–4000 cm^{−1}. Each sample was ground with KBr at an approximate ratio of 1:200 and the resulting mixture was then pressed. The background obtained from a scan of pure KBr was automatically subtracted from the sample spectra. The pH of point of zero charge (pH_{pzc}) of the PKOH chips was assessed following the procedure earlier depicted in detail for PNAT chips, in our previous study (Fernandez et al., 2010).

N₂ adsorption–desorption isotherms at −196 °C for PNAT and PKOH chips were determined with an automatic Micromeritics ASAP-2020 HV volumetric sorption analyzer. Prior to gas adsorption measurements, the samples were outgassed at 60 °C for three hours. Textural properties were assessed from the isotherms, according to conventional procedures depicted in detail in previous studies (de Celis et al., 2009; Ramos et al., 2011). The Brunauer–Emmett–Teller (BET) surface area (*S*_{BET}) was determined by the standard BET procedure and total pore volumes (*V*_t) were estimated from the amount of nitrogen adsorbed at the relative pressure of 0.95 (*p/p*₀ = 0.95).

2.3. Batch biosorption from single-dye-solutions on PKOH

Stock solutions of 2.1 mmol/L were prepared by dissolving the necessary amount of methylene blue and rhodamine B in distilled water and diluted to obtain the desired concentrations of the dyes. Biosorption experiments were carried out using capped Erlenmeyer flasks in a batch thermostated system (Lauda Ecoline E200) at 20 ± 0.5 °C, under a wrist-action shaker agitation at a constant speed of 250 rpm up to biosorption equilibrium. Afterward, all samples were centrifuged for 10 min at 5000 rpm and the concentration of each dye was calculated according to the Beer Lambert's law from the measured absorbance in the supernatant at their corresponding maximum absorption wavelength (*λ*_{max}MB = 663 nm and *λ*_{max}RhB = 553 nm) employing an UV–Vis spectrophotometer (Shimadzu Model UV mini 1240).

The pH effect on dyes biosorption was studied in the range 2–8. This range was chosen because over pH 9, color leaching was evidenced in the blanks. Dye solutions of pH 8 were prepared using Na/K phosphates buffer, because it was difficult to maintain this pH value throughout the experiments duration. Solutions of the remaining pH were prepared with distilled water and adjusted with HCl and NaOH solutions. Amounts of 0.05 g and 0.1 g of PKOH were contacted with 100 mL of 0.21 mmol/L MB and RhB solutions, respectively, for 48 h to ensure equilibrium. Dyes removal percentages were calculated as follows:

$$\text{Removal (\%)} = 100 \left(\frac{C_0 - C_e}{C_0} \right) \quad (1)$$

where *C*₀ and *C*_e are the initial and equilibrium dye concentrations (mmol/L) in solution, respectively.

Equilibrium biosorption isotherms were obtained by contacting 100 mL of different initial concentrations (0.08–2.0 mmol/L) of MB and RhB solutions with 0.1 and 0.2 g of the biosorbent, respectively,

until equilibrium was attained. The same temperature and agitation conditions aforementioned, as well as the pH selected from the pH effect experiments were employed. The amount of dye biosorbed per gram of biosorbent at equilibrium, q_e (mmol/g), was calculated as follows:

$$q_e = \frac{(C_0 - C_e)V}{m} \quad (2)$$

where C_0 is the initial concentration of the dye in the solution (mmol/L), C_e , the equilibrium concentration of the dye in the solution (mmol/L), V , the volume of solution (L), and m , the mass of biosorbent used (g).

Kinetic experiments using single-dye solutions were performed by agitating 0.2 g of the PKOH chips with 100 mL of 0.21 mmol/L MB and RhB solutions, individually, at a constant speed of 250 rpm and a controlled temperature of 20 ± 0.5 °C, keeping otherwise the same conditions detailed above. In each case, the pH of the solution was selected as the optimum from the pH effect experiments. Samples were withdrawn at appropriate time intervals and absorbance in the supernatant was measured. Preliminary experiments with both average particle sizes were done to examine possible external and intraparticle mass transfer resistances.

All biosorption experiments were performed at least twice. Average values are reported. Solute and biosorbent blanks, at the corresponding pH, were simultaneously run under the same conditions to account for any color leached by the biosorbent.

2.4. Competitive kinetics of dyes biosorption on PNAT and PKOH

Competition between methylene blue and rhodamine B for the biosorption onto the surface of the unmodified (PNAT) and modified (PKOH) cypress cone chips was examined from batch kinetic experiments, agitating 0.2 g of each given biosorbent with 100 mL of a binary solution with 0.21 mmol/L of both dyes, until equilibrium. For the sake of comparison, biosorption was conducted at both optimum pH values selected from the pH effect experiments. The remaining operating conditions were kept identical to those applied for kinetic experiments using single-dye solutions.

2.5. Dynamic biosorption for single and binary dyes solutions

For continuous biosorption experiments, an acrylic column (1.6 cm internal diameter and 34 cm height) was packed with a known mass of each biosorbent. Prior to the measurements, the bed was washed with distilled water in order to remove all interstitial air. To complete the volume of the column, glass beads were also packed and metallic sieves in the extremes were used to avoid losses of material.

The column was then fed with single or binary solutions of MB and RhB of a known concentration (0.21 mmol/L) for each dye, in up-flow mode. The pH for each dye was selected from batch experiments. Dyes solutions were prepared using buffers Na/K phosphates for experiments at pH 7 and acetic acid/Na acetate for experiments at pH 4, in order to maintain constant pH throughout the runs. Previously, best conditions for the biosorbent's behavior in dynamic mode was studied for PNAT, varying particle diameter, bed depth and flow rate. Single and binary solutions experiments using PNAT and PKOH were performed choosing the best conditions, determined from these experiments. A flow rate of 11 mL/min was adjusted using a peristaltic pump (Masterflex 1–100 rpm, Cole-Parmer) with a flow controller. Samples were collected at the exit of the column at desired time intervals, using a solenoid valve and an automatic sample collector; the dye concentrations were analyzed spectrophotometrically. As earlier described, all the experiments were carried out at 20 ± 0.5 °C using

a thermostated system (Lauda Ecoline E 300). Temperature was further monitored by an internal thermocouple connected to a digital controller (Iea, Micro 80).

The breakthrough time t_b (the time at which the dye concentration in the effluent reached 5% of the influent concentration) and the exhaustion time t_e (the time at which the dye concentration in the effluent reached 95% of the influent concentration) were determined to characterize the breakthrough curves (Al-Degs et al., 2009; Kumar and Chakraborty, 2009; Vijayaraghavan and Yun, 2008).

3. Results and discussion

3.1. Characterization of cone chips

The effect of the treatment with potassium hydroxide on cypress cone chips was determined by investigating changes in physicochemical and textural characteristics of the material. A weight-loss of 24% was obtained due to the treatment. The color of the liquid at the end of the experiment was dark brown, indicating that pigments and lipids were removed (Ofomaja and Naidoo, 2010). Table 1 shows comparatively the physicochemical characteristics for the unmodified (PNAT) and modified (PKOH) cypress cone chips. Contents of volatile matter and fixed carbon obtained from the proximate analysis of PKOH as well as percentages of C, H, N, and O were very similar to those determined for PNAT in our previous work (Fernandez et al., 2010) and the results reported for other conifer cones (Font et al., 2009). A slight decrease in the percentage of elemental and fixed carbon was appreciated in PKOH along with an increase in the oxygen content. The treatment changed the proportion of functional groups present on the biosorbent; polar/acidic oxygen functional groups decreased in PKOH along with the introduction of more basic groups on its surface. In agreement with Ofomaja and Naidoo (2010), changes in total acidity and basicity affect the pH_{pzc} of the biosorbent as corroborated from the rise of pH_{pzc} value after the alkaline modification of the material. Because the net surface charge of the biosorbent is negative when the pH of the solution is over the pH_{pzc} , and positive when it is below the pH_{pzc} , biosorption of positively charged molecules, such as cationic dyes, may be favored.

FT-IR spectra of the unmodified and modified samples, displayed in Fig. S1 (provided as Supplementary Data) were quite similar, showing characteristic peaks also reported by other authors for conifer cones (Akar et al., 2009). Numerous peaks were

Table 1

Chemical characteristics of unmodified (PNAT) and modified (PKOH) cypress cone chips: pH of point of zero charge (pH_{pzc}), total content of polar/acidic oxygen functional groups (TOFG), total basic groups (TBG) and proximate and ultimate analyses.

	PNAT ^a	PKOH
pH_{pzc}	6.1	6.7
TOFG [mequiv./g]	1.5	1.0
TBG [mequiv./g]	0.5	1.0
<i>Proximate analysis [wt.%, dry basis]</i>		
Volatile matter	65.0	67.1
Ash	6.5	5.4
Fixed carbon ^b	28.5	27.5
<i>Ultimate analysis [wt.%, dry and ash-free basis]</i>		
Carbon	52.9	49.2
Hydrogen	6.0	5.7
Nitrogen	2.3	1.0
Sulfur	0.0	0.0
Oxygen ^b	38.8	44.0

^a Fernandez et al. (2010).

^b Estimated by difference.

appreciated indicating the complex nature of the material, with the same functional groups observed in both spectra. These included an intense broad absorption peak around 3390 cm^{-1} which represents the stretching vibrations of hydroxyl groups from polymeric compounds such as cellulose, hemicelluloses and lignin and chemisorbed water. A well-defined peak at 2920 cm^{-1} was also found, corresponding to the C–H stretching of the CH_2 groups. According to Min et al. (2004), the region between 1500 and 1800 cm^{-1} is especially adequate for evaluating the degree of saponification since this is the carbonyl and double-bond region. One of the major differences between the samples is the presence of a peak around 1713 cm^{-1} in PNAT, attributed to stretching vibrations of C=O in esters and carboxylic acids groups which was absent in the modified biosorbent. The other major peak was obtained in both spectra at 1620 cm^{-1} corresponding to carboxylate groups. The intensity of the latter peak in PKOH was found to be intensified, suggesting an increase in the amount of these groups as a result of the saponification produced by the alkaline treatment. This finding is analogous to the results obtained by Min et al. (2004).

Textural parameters evaluated from isotherms analysis by the Brunauer–Emmett–Teller (BET) showed negligible BET surfaces areas ($S_{\text{BET PNAT}} = 1.1\text{ m}^2/\text{g}$, $S_{\text{BET PKOH}} = 1\text{ m}^2/\text{g}$) and total pore volume ($V_{\text{T PNAT}} = 11 \times 10^{-4}\text{ cm}^3/\text{g}$, $V_{\text{T PKOH}} = 9 \times 10^{-4}\text{ cm}^3/\text{g}$). This indicated that the alkaline treatment practically unaltered textural characteristics of the pristine cone chips.

3.2. Batch biosorption from single-dye-solutions on PKOH

The effect of the solution pH on the biosorption of MB and RhB using PKOH was investigated. Fig. 1 conclusively shows that the increase of the solution pH led to an increase in the biosorption of MB and a decrease in the biosorption of RhB. These tendencies were also observed by Fernandez et al. (2010) using PNAT. These results could be explained in terms of the value of pH_{pzc} determined for PKOH and of the molecular form of the dyes at each pH considered. For methylene blue, at $\text{pH} \geq \text{pH}_{\text{pzc}}$ the negatively charged surface of PKOH likely intensifies the electrostatic attraction to the positively charged dye; furthermore, the lower biosorption at acidic pH may be due to the presence of an excess of H^+ ions which compete with the dye cation for biosorption sites (Batzias and Sidiras, 2004). Although ion exchange was suggested as the main mechanism involved in MB biosorption (Fernandez et al.,

2010; Janoš et al., 2009), other mechanism could also occur since the enhanced value of the pH_{pzc} of PKOH, which indicates a lower negative surface charge than that of PNAT, did not lead to decrease the biosorption of this dye, in comparison with previously reported MB biosorption on PNAT (Fernandez et al., 2010). This idea is reinforced by the very low desorption obtained for both dyes in our previous work (Fernandez et al., 2010). On the other hand, biosorption of rhodamine B was also enhanced using PKOH with respect to PNAT (Fernandez et al., 2010). The intensified biosorption at lower pH may be a consequence of the formation of RhB cations in an excess of H^+ ions, by neutralization of the anionic group of the zwitterionic molecular form of RhB, leaving only the positive charge with affinity to negatively charged surfaces. Additionally, aggregation of the zwitterionic form of RhB reportedly occurs at $\text{pH} > 4$, generating dimers which could hinder the biosorption onto the surface of the chips (Gad and El Sayed, 2009). Based on the highest removal percentages achieved, values of pH 4 for RhB, and pH 7 for MB were selected for the batch and continuous experiments.

Experimental isotherms for the biosorption of MB and RhB onto PKOH are shown in Fig. 2. Three different sorption models were comparatively applied for data fitting. The Langmuir model, which assumes monolayer coverage and identical sites with the same adsorption energy on the sorbent surface, is described by the following equation:

$$q_e = \frac{K_L q_{\text{mL}} C_e}{1 + K_L C_e} \quad (3)$$

where q_e is the molar amount of the dye sorbed at equilibrium per mass sample unit (mmol/g), K_L , the Langmuir constant related to the energy of adsorption (L/mmol) and q_{mL} , the maximum amount of sorption corresponding to complete monolayer coverage on the surface (mmol/g). The Freundlich model, which assumes sorption onto heterogeneous solid surface and adsorption energy sites of exponential type, is represented by

$$q_e = K_F C_e^{\eta_F} \quad (4)$$

where K_F and η_F are the Freundlich isotherm constants related to biosorption capacity and intensity, respectively. Finally, a combination of the two previous models, known as the Langmuir–Freundlich equation (Janoš et al., 2009) and defined by Eq. (5), was applied:

$$q_e = \frac{K_{\text{LF}} q_{\text{mLF}} C_e^{\eta_{\text{LF}}}}{1 + K_{\text{LF}} C_e^{\eta_{\text{LF}}}} \quad (5)$$

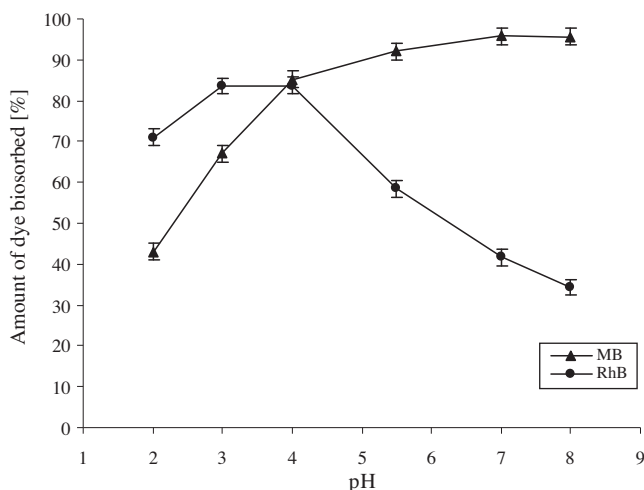


Fig. 1. Effect of the solution's pH on biosorption of methylene blue (MB) and rhodamine B (RhB) for PKOH at equilibrium. $C_0 = 0.21\text{ mmol/L}$; doses: $0.05\text{ g}/100\text{ mL}$ (MB) and $0.1\text{ g}/100\text{ mL}$ (RhB).

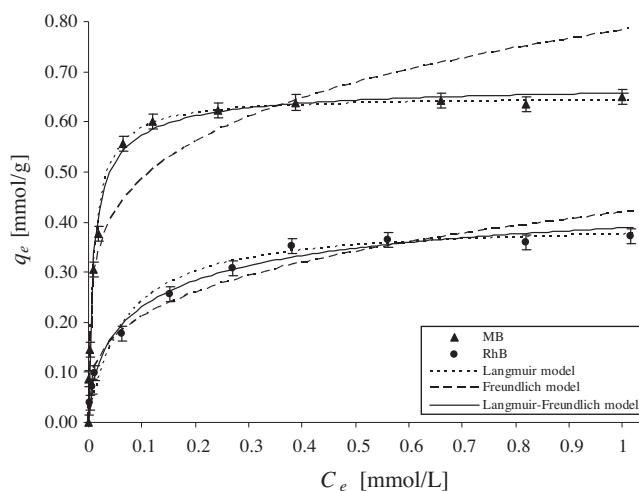


Fig. 2. Equilibrium isotherms for methylene blue (MB) and rhodamine B (RhB) onto PKOH. Comparison between the experimental data (points) and predictions of the Langmuir, Freundlich and Langmuir–Freundlich models (lines). $C_0 = 0.05\text{--}1.5\text{ mmol/L}$ at pH 7 (MB) and pH 4 (RhB); doses: $0.1\text{ g}/100\text{ mL}$ (MB) and $0.2\text{ g}/100\text{ mL}$ (RhB).

where q_e is the molar amount of the dye sorbed at equilibrium per mass sample unit (mmol/g), q_{mLF} , the maximum amount of sorption (mmol/g), K_{LF} , the Langmuir–Freundlich constant (L/mmol) and n_{LF} , an additional parameter which characterizes the system heterogeneity arisen from the biosorbent, the contaminant or a combination of both. Table 2 presents characteristic parameters of the models for the biosorption of MB and RhB onto PKOH which were estimated by non-linear regression analysis for a 5% significance level, by minimizing the following objective function (O.F.):

$$\text{O.F.} = \sum (q_{\text{exp}} - q_{\text{mod}})^2 \quad (6)$$

The tested biosorbent exhibited higher biosorption ability for MB than for RhB. The resulting isotherms (Fig. 2) were concave showing a saturation trend at higher dye concentrations. The Langmuir–Freundlich model fitted data extremely well ($R > 0.99$), although high correlation coefficients were also obtained with the Langmuir model applied to both dyes biosorption, especially for MB, indicating monolayer coverage of PKOH surface. A large difference in the intensity of the biosorption is inferred from the K_L and K_{LF} values, being these parameters six and eight times larger for MB biosorption than for rhodamine B one, respectively. The Freundlich model exhibited a less appropriate fit. As observed in Table 2, maximum biosorption capacities for PKOH evaluated according to Langmuir model, increased around 5% for MB and 67% for RhB in comparison with those for PNAT reported earlier (Fernandez et al., 2010), demonstrating that the treatment of the cone chips with alkaline hydroxide improved the biosorption ability for both dyes. Biosorption capacity for MB is comparable to the highest values listed in the recent review by Rafatullah et al. (2010) for agricultural solid wastes.

Kinetic data for the biosorption of both dyes from single solutions using PKOH are illustrated in Fig. 3(a). As seen, removal rates were very fast for both dyes during the initial stages of the biosorption process and slowed gradually as equilibrium was approached. This could be associated to the reduction of available active sites on the biosorbent. A pseudo-second-order rate model (Ho, 2006) was applied in order to describe the biosorption kinetics:

$$q_t = \frac{q_{\text{eH}}^2 k_H t}{1 + q_{\text{eH}} k_H t} \quad (7)$$

where q_t is the amount of dye biosorbed at any time t (mmol/g), k_H , the rate constant of biosorption (g/mmol min) and q_{eH} , the amount of dye biosorbed at equilibrium per unit mass of biosorbent (mmol/g). Table 3 summarizes the model parameters for the biosorption of

Table 2
Model parameters estimated for the sorption isotherms of methylene blue (MB) and rhodamine B (RhB) onto PKOH, along with their corresponding standard errors.

	MB	RhB
<i>Langmuir parameters</i>		
q_{mL} [mmol/g]	0.65 ± 0.02	0.40 ± 0.02
K_L [L/mmol]	95.1 ± 13.4	15.2 ± 4.3
r^2	0.989	0.965
SEE [mmol/L]	0.03	0.03
<i>Freundlich parameters</i>		
n_F	0.21 ± 0.03	0.30 ± 0.03
K_F [(mmol/g)(L/mmol) n_F]	0.78 ± 0.06	0.42 ± 0.02
r^2	0.934	0.957
SEE [mmol/L]	0.07	0.03
<i>Langmuir–Freundlich parameters</i>		
q_{mLF} [mmol/g]	0.68 ± 0.02	0.50 ± 0.06
K_{LF} [(L/mmol) $^{n_{LF}}$]	29.2 ± 7.7	3.6 ± 1.6
n_{LF}	0.73 ± 0.06	0.62 ± 0.08
r^2	0.995	0.991
SEE [mmol/L]	0.02	0.01

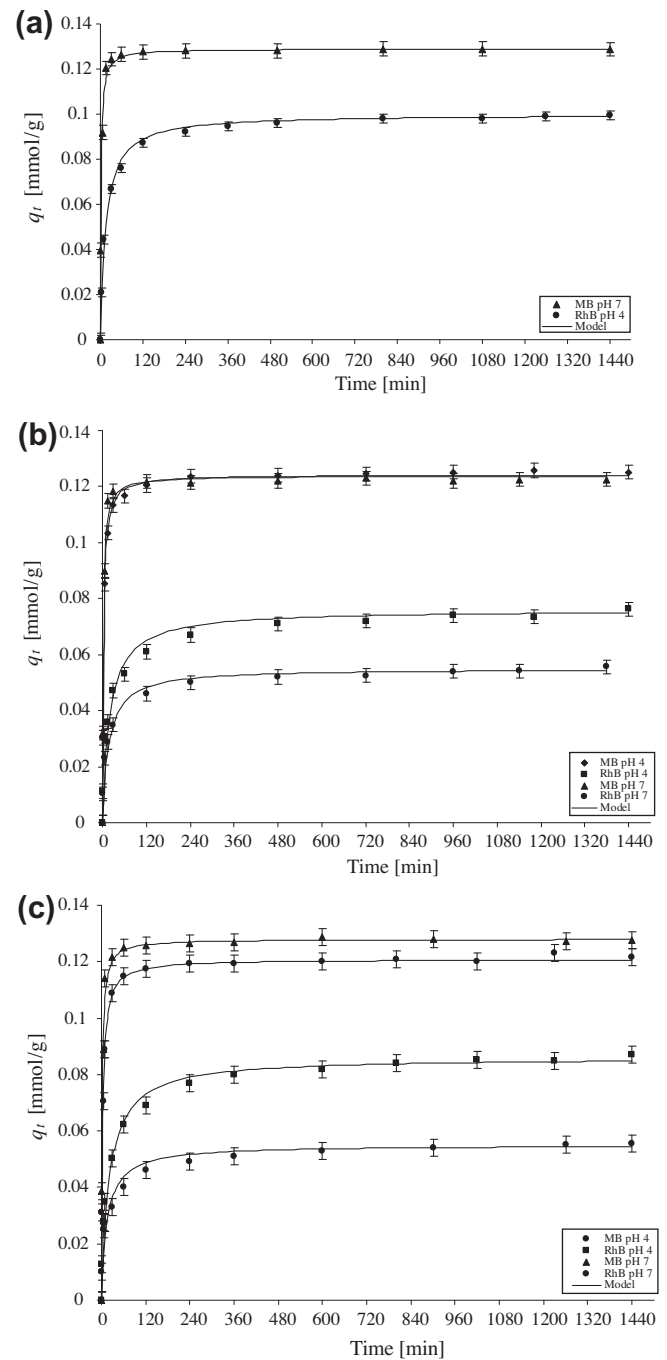


Fig. 3. Kinetic data for biosorption from: (a) single solutions of methylene blue (MB) and rhodamine B (RhB) onto PKOH; (b) binary solutions of the dyes onto PNAT, and (c) binary solutions of the dyes onto PKOH. Comparison between the experimental data (points) and predictions of the pseudo-second-order rate model (lines). $C_0 = 0.21$ mmol/L of each dye at pH 7 (MB) and pH 4 (RhB); dose = 0.2 g/100 mL.

both dyes which were also estimated by non-linear regression analysis for a 5% significance level, as detailed earlier (Eq. (6)).

The rate constant estimated for MB biosorption was one order of magnitude and about six times higher than that for RhB biosorption. These values are similar to those obtained for PNAT (Fernandez et al., 2010). As may be observed in Fig. 3(a), the kinetic model enabled to describe properly the experimental data with high correlation coefficients ($r^2 > 0.98$) and low standard errors of the estimate (SEE).

Table 3

Estimated parameters of the pseudo-second-order kinetic model for the biosorption of methylene blue (MB) and rhodamine B (RhB) from: single-dye solutions onto PKOH; binary solutions of the dyes onto PNAT, and binary solutions of the dyes onto PKOH, along with their corresponding standard errors.

	pH	Dye	q_{eH} [mmol/g]	k_H [g/mmol min]	r^2	SEE [mmol/g]
<i>Single-dye solutions</i>						
PKOH	7	MB	0.129 ± 0.001	4.3 ± 0.3	0.995	0.004
	4	RhB	0.10 ± 0.02	0.7 ± 0.1	0.989	0.004
<i>Binary solutions</i>						
PNAT	7	MB	0.124 ± 0.002	4.1 ± 0.4	0.992	0.004
		RhB	0.055 ± 0.002	1.1 ± 0.5	0.944	0.005
	4	MB	0.124 ± 0.001	3.0 ± 0.2	0.997	0.002
		RhB	0.076 ± 0.003	0.7 ± 0.3	0.941	0.007
PKOH	7	MB	0.128 ± 0.001	4.1 ± 0.3	0.995	0.003
		RhB	0.055 ± 0.002	1.2 ± 0.6	0.926	0.005
	4	MB	0.121 ± 0.001	2.46 ± 0.09	0.999	0.002
		RhB	0.086 ± 0.002	0.6 ± 0.2	0.954	0.006

3.3. Competitive kinetics of dyes biosorption on PNAT and PKOH

In order to determine the biosorption effectiveness in a more complex system, the interaction between the dyes chosen and the biosorbent applicability to continuous effluent treatment, competitive kinetics of both dyes biosorption on PNAT and PKOH was investigated. The results are illustrated in Fig. 3(b) and (c), respectively. As seen, removal from binary solutions shows the same trend as from single-dye solutions. The same pseudo-second-order rate model (Eq. (7)) was applied in order to describe the competitive kinetics. Fig. 3(b) and (c) show that this model enabled to describe properly the experimental data with very high correlation coefficients for MB ($r^2 > 0.99$) at both pH and using both materials, although a rather less appropriate fit to the experimental data was obtained for RhB.

Characteristic parameters were also estimated by non-linear regression analysis (Eq. (6)) and they are also presented in Table 3. Preferential MB biosorption still held when both dyes are simultaneously present in the solution, as can be inferred from greater kinetic rate constants. Values achieved for MB in competitive biosorption with PNAT and PKOH were analogous to those obtained in single-MB biosorption at the optimum condition for MB (pH 7), while smaller k_H were attained at a less favorable pH. These results suggest that MB biosorption was not influenced by the presence of RhB in the solution. In contrast, the achieved parameters for RhB show diminished q_{eH} at both pH values and with both biosorbents, indicating a competition with MB for some of the available surface sites and the detrimental effect that MB produced on RhB biosorption. At the less favorable condition (pH 7) both biosorbents' saturations with RhB were faster, as inferred from k_H , regardless of the decrease in q_{eH} . Recent results by other authors for multi-dyes mixtures also confirm that competition for the limited binding sites in the solid reduces the efficiency of the contaminants removal (Gao et al., 2011; Yang et al., 2011).

3.4. Dynamic biosorption of single and binary dyes system solutions

Results obtained for MB and RhB single-dye biosorption onto PKOH are illustrated in Fig. 4 and compared with those previously obtained for these dyes onto PNAT (Fernandez et al., 2010). Breakthrough curves in the figure are expressed in terms of normalized concentration, defined as the ratio of effluent dye concentration to influent dye concentration (C_{ef}/C_{in}), as a function of time (t). As can be observed, breakthrough curves maintained the typical S-shapes and the tailing near exhaustion time as originally obtained for the unmodified biosorbent. However, breakthrough occurred at more prolonged times (t_b), for both dyes, indicating enhanced removal

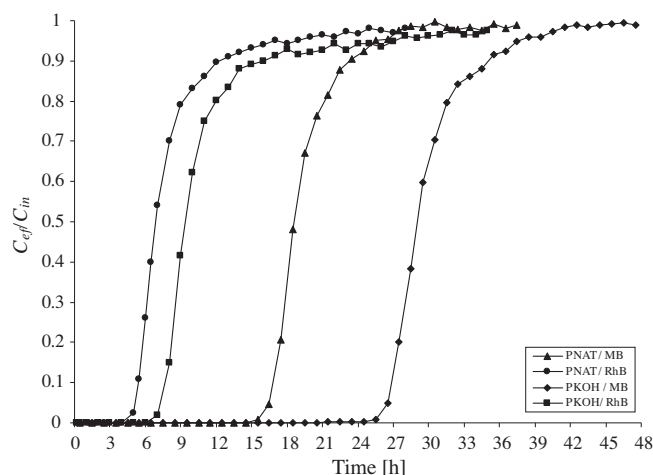


Fig. 4. Breakthrough curves obtained for dynamic single-dye biosorption of methylene blue (MB) and rhodamine B (RhB) onto PKOH. $C_{in} = 0.21$ mmol/L at pH 7 (MB) and pH 4 (RhB). Load of biosorbent: 6 g. Comparison with the breakthrough curves for the same dyes and conditions onto PNAT (Fernandez et al., 2010).

efficiencies. Breakthrough times increased around 40% for RhB and 60% for MB.

For a better description of the breakthrough curves, performance parameters were calculated (Kumar and Chakraborty, 2009; Vijayaraghavan and Yun, 2008). Length of the mass transfer zone (L_m) was calculated using the breakthrough and exhaustion times along with the total bed depth (L):

$$L_m = L \left(1 - \frac{t_b}{t_e} \right) \quad (8)$$

Mass of dye removed (M_r) was calculated based on the difference between the influent dye load, calculated from throughput volume (V_{ex}) at column exhaustion and influent dye concentration (C_{in}), and the mass of dye not removed, as obtained from the area below the breakthrough curve, according to:

$$M_r = (V_{ex} \cdot C_{in}) - \sum \left[\frac{(V_{n+1} - V_n)(C_{n+1} + C_n)}{2} \right] \quad (9)$$

where V_n is the throughput volume at n th reading (L), V_{n+1} , the throughput volume at $(n+1)$ th reading (L), C_n , the effluent dye concentration at n th reading (mmol/L), and C_{n+1} , the effluent dye concentration at $(n+1)$ th reading (mmol/L).

Finally, dye uptake (q_c) at exhaustion time, expressed in mmol/g, was calculated as follows:

$$q_c = \frac{M_r}{\text{biosorbent mass}} \quad (10)$$

Single-dye dynamic performance parameters for PNAT and PKOH are presented in Table 4. For both dyes, no considerable change in L_m was observed as a consequence of the alkaline treatment of the chips. Mass transfer zones indubitably remain shorter for MB, given their L_m values reached only one third of the total bed depth, while for RhB they reached more than two thirds of it. Column capacities at 95% of exhaustion, using PKOH increased about 50% in relation to PNAT for both dyes. For RhB, this increase agrees with the enhanced capacity obtained from batch equilibrium experiments (q_{mL}) although a less efficient use of this capacity was found. It may be attributed to the slower kinetics and to the insufficient contact time between the solute and the biosorbent in the column (Tan et al., 2008). In contrast, column capacity for MB turned up to be much higher than maximum batch capacity. According to Gupta et al. (2004), a higher column capacity can result from a large concentration gradient continuously present

Table 4

Performance parameters for the biosorption of methylene blue (MB) and rhodamine B (RhB) by the untreated and the modified cone chips from single-dye solutions in continuous mode: breakthrough time (t_b), exhaustion time (t_e), length of the mass transfer zone (L_m), mass of dye removed (M_r) and dye uptake at exhaustion time (q_c). $C_{in} = 0.21$ mmol/L at pH 7 (MB) and pH 4 (RhB). Load of biosorbent: 6 g. Flow rate: 11 mL/min.

Biosorbent	Dye	t_b [h]	t_e [h]	L_m [cm]	M_r [mmol]	q_c [mmol/g]
PNAT ^a	MB (pH 7)	16.5	25.5	3.5	3.02	0.503
	RhB (pH 4)	5.1	17.0	7.0	1.00	0.167
PKOH	MB (pH 7)	26.5	37.5	2.9	4.50	0.750
	RhB (pH 4)	7.2	27.2	7.4	1.51	0.251

^a Fernandez et al. (2010).

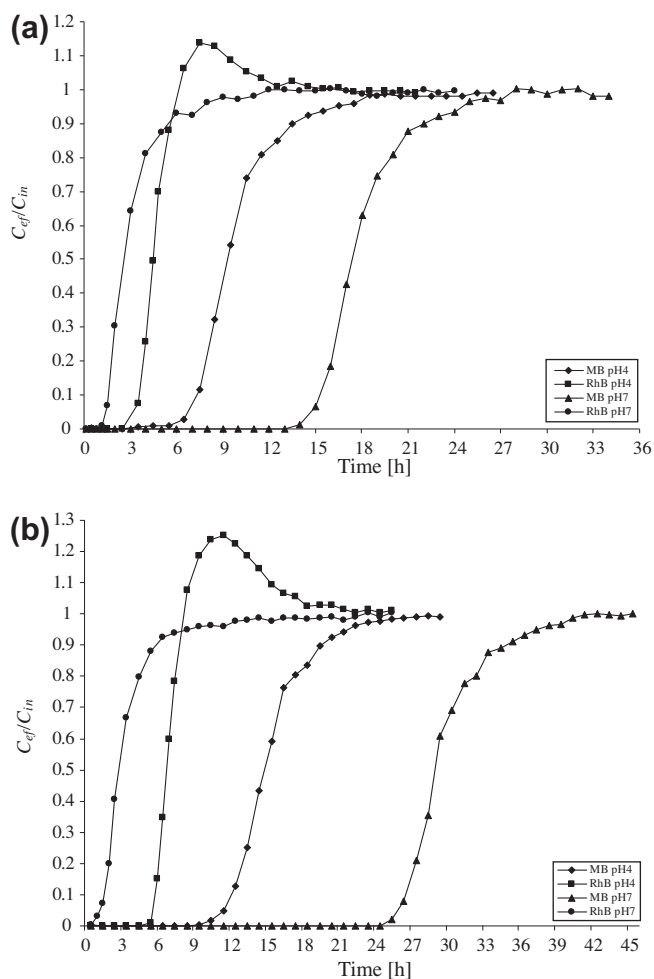


Fig. 5. Breakthrough curves obtained for dynamic binary-dye biosorption of methylene blue (MB) and rhodamine B (RhB) onto: (a) PNAT; (b) PKOH. Comparison between solutions of pH 4 and pH 7. $C_{in} = 0.21$ mmol/L of each dye. Load of biosorbent: 6 g.

at the interface zone as the dye solution passes through the column, whereas the concentration gradient decreases with time in batch experiments.

The applicability of a biosorbent for real wastewater treatment requires knowledge of its behavior in continuous systems with more than a single contaminant. Results obtained for MB and RhB competitive biosorption onto PNAT and PKOH are illustrated in Fig. 5(a) and (b), respectively. Performance parameters for dyes binary systems were also calculated, following Eqs. (8)–(10) they are presented in Table 5.

In agreement with kinetic batch experiments, the continuous mode biosorption of MB from a binary solution was not especially affected. Although t_b was found slightly lower for PNAT, exhaustion

Table 5

Performance parameters for the biosorption of methylene blue (MB) and rhodamine B (RhB) in continuous mode from binary solutions: breakthrough time (t_b), exhaustion time (t_e), length of the mass transfer zone (L_m), mass of dye removed (M_r) and dye uptake at exhaustion time (q_c). Comparison between binary solutions at pH 4 and pH 7. $C_{in} = 0.21$ mmol/L of each dye. Load of biosorbent: 6 g. Flow rate: 11 mL/min.

Biosorbent	pH	Dye	t_b [h]	t_e [h]	L_m [cm]	M_r [mmol]	q_c [mmol/g]
PNAT	7	MB	14.7	24.7	4.0	2.99	0.499
		RhB	1.4	7.7	8.2	0.59	0.099
	4	MB	6.7	16.3	5.9	1.48	0.247
		RhB	3.2	5.9	4.6	0.57	0.094
PKOH	7	MB	26.0	37.5	3.1	4.51	0.752
		RhB	1.1	8.5	8.7	0.34	0.057
	4	MB	11.5	21.9	4.8	2.30	0.383
		RhB	5.6	8.1	3.0	0.92	0.154

times and column capacities obtained for both biosorbents remain almost the same as those for single-dye column experiments. Reductions in breakthrough and exhaustion times and column capacities were also appreciated for MB biosorption at the least favorable condition (pH 4), as a consequence of the strong influence of pH not only on the charge of the surface active sites on PNAT and PKOH but also on the biosorption availability for the dyes and the charge of the dye molecules. A similar influence was verified for RhB at its least favorable condition (pH 7).

Interestingly, an overshoot region is observed in the two curves (Fig. 5) that represent RhB biosorption with PNAT and PKOH at pH 4, reaching concentrations 15% and 25% higher than the influent concentration. This behavior suggests that initially bonded RhB molecules are displaced by MB molecules due to the higher affinity of the latter for the active surface sites. Similar observations for metal ions (Naja and Volesky, 2006; Vilar et al., 2009) and for mixtures of 1,2-cis-dichloroethene and trichloroethene (Salaices Avila and Breiter, 2008) have been reported in literature. Moreover, as a result of the competitive exchange, RhB overshoots considerably before the exhaustion time, reducing the L_m along with the service time and capacity of the column. Additionally, in the absence of competition, large biosorbed molecules are more unlikely to desorb since they might have several contact points with the biosorbent surface (Janoš et al., 2009), which may be reduced in the presence of another molecule with greater affinity.

4. Conclusions

Present results demonstrate that a simple modification of a forest residue improves its performance as biosorbent for basic dyes. Enhanced maximum biosorption capacities for both dyes were elucidated from modeling of the equilibrium isotherms obtained in batch mode. Pseudo-second-order kinetics adequately described the biosorption process from single and binary solutions. Dynamic experiments allowed the identification of a reduced biosorption of the dye with the weakest affinity for the active sites of

the biosorbent. This reinforces the mandatory need of dynamic studies with mixtures of contaminants to attain a proper approach to the applicability of a biosorbent for large-scale wastewater treatment.

Acknowledgements

The authors gratefully acknowledge Consejo Nacional de Investigaciones Científicas y Técnicas (CONICET) and Universidad de Buenos Aires (UBA) from Argentina, for financial support.

Appendix A. Supplementary data

Supplementary data associated with this article can be found, in the online version, at [doi:10.1016/j.biortech.2011.12.003](https://doi.org/10.1016/j.biortech.2011.12.003).

References

- Akar, T., Divriklioglu, M., 2010. Biosorption applications of modified fungal biomass for decolorization of reactive red 2 contaminated solutions: batch and dynamic flow mode studies. *Bioresour. Technol.* 101, 7271–7277.
- Akar, T., Ozcan, A.S., Tunali, S., Ozcan, A., 2008. Biosorption of a textile dye (acid blue 40) by cone biomass of *Thuja orientalis*: estimation of equilibrium, thermodynamic and kinetic parameters. *Bioresour. Technol.* 99, 3057–3065.
- Akar, S.T., Gorgulu, A., Kaynak, Z., Anilan, B., Akar, T., 2009. Biosorption of reactive blue 49 dye under batch and continuous mode using a mixed biosorbent of macro-fungus *Agaricus bisporus* and *Thuja orientalis* cones. *Chem. Eng. J.* 148, 26–34.
- Al-Degs, Y.S., Khraisheh, M.A.M., Allen, S.J., Ahmad, M.N., 2009. Adsorption characteristics of reactive dyes in columns of activated carbon. *J. Hazard. Mater.* 165, 944–949.
- Anastasi, A., Spina, F., Prigione, V., Tigini, V., Giansanti, P., Varese, G.C., 2010. Scale-up of a bioprocess for textile wastewater treatment using *Bjerkandera adusta*. *Bioresour. Technol.* 101, 3067–3075.
- Attia, A.A., Girgis, B.S., Khedr, S.A., 2003. Capacity of activated carbon derived from pistachio shells by H_3PO_4 in the removal of dyes and phenolics. *J. Chem. Technol. Biotechnol.* 78, 611–619.
- Basso, M.C., Cerrella, E.G., Cukierman, A.L., 2002. Lignocellulosic materials as potential biosorbents of trace toxic metals from wastewater. *Ind. Eng. Chem. Res.* 41, 3580–3585.
- Batzias, F.A., Sidiras, D.K., 2004. Dye adsorption by calcium chloride treated beech sawdust in batch and fixed-bed systems. *J. Hazard. Mater.* 114, 167–174.
- De Celis, J., Amadeo, N.E., Cukierman, A.L., 2009. In situ modification of activated carbons developed from a native invasive wood on removal of trace toxic metals from wastewater. *J. Hazard. Mater.* 161, 217–223.
- Drnovšek, T., Perdih, A., 2005. Selective staining as a tool for wood fibre characterization. *Dyes Pigm.* 67, 197–206.
- Fernandez, M.E., Nunell, G.V., Bonelli, P.R., Cukierman, A.L., 2010. Effectiveness of *Cupressus sempervirens* cones as biosorbent for the removal of basic dyes from aqueous solutions in batch and dynamic modes. *Bioresour. Technol.* 101, 9500–9507.
- Font, R., Conesa, J.A., Moltó, J., Muñoz, M., 2009. Kinetics of pyrolysis and combustion of pine needles and cones. *J. Anal. Appl. Pyrolysis* 85, 276–286.
- Forgacs, E., Cserháti, T., Oros, G., 2004. Removal of synthetic dyes from wastewaters: a review. *Environ. Int.* 30, 953–971.
- Gad, H.M.H., El Sayed, A.A., 2009. Activated carbon from agricultural by-products for the removal of rhodamine-B from aqueous solution. *J. Hazard. Mater.* 168, 1070–1081.
- Gao, J.F., Wang, J.H., Yang, C., Wang, S.Y., Peng, Y.Z., 2011. Binary biosorption of acid red 14 and reactive red 15 onto acid treated okara: simultaneous spectrophotometric determination of two dyes using partial least squares regression. *Chem. Eng. J.* 171, 967–975.
- Gupta, V.K., Suhas, 2009. Application of low-cost adsorbents for dye removal – a review. *J. Environ. Manage.* 90, 2313–2342.
- Gupta, V.K., Suhas, Ali, I., Saini, V.K., 2004. Removal of rhodamine B, fast Green, and methylene blue from wastewater using red mud, an aluminum industry waste. *Ind. Eng. Chem. Res.* 43, 1740–1747.
- Ho, Y.S., 2006. Review of second-order models for adsorption systems. *J. Hazard. Mater.* 136, 681–689.
- Janoš, P., Coskun, S., Pilařová, V., Rejnek, J., 2009. Removal of basic (methylene blue) and acid (egacid orange) dyes from waters by sorption on chemically treated wood shavings. *Bioresour. Technol.* 100, 1450–1453.
- Kumar, P.A., Chakraborty, S., 2009. Fixed-bed column study for hexavalent chromium removal and recovery by short-chain polyaniline synthesized on jute fiber. *J. Hazard. Mater.* 162, 1086–1098.
- Min, S.H., Han, J.S., Shin, E.W., Park, J.K., 2004. Improvement of cadmium ion removal by base treatment of juniper fiber. *Water Res.* 38, 1289–1295.
- Naja, G., Volesky, B., 2006. Multi-metal biosorption in a fixed-bed flow-through column. *Colloids Surf. A: Physicochem. Eng. Aspects* 281, 194–201.
- Nigam, P., Armour, G., Banat, I.M., Singh, D., Marchant, R., McHale, A.P., McMullan, G., 2000. Physical removal of textile dyes from effluents and solid-state fermentation of dye-adsorbed agricultural residues. *Bioresour. Technol.* 72 (3), 219–226.
- Ofomaja, A.E., Naidoo, E.B., 2010. Biosorption of lead(II) onto pine cone powder: studies on biosorption performance and process design to minimize biosorbent mass. *Carbohydr. Polym.* 82, 1031–1042.
- Panda, G.C., Das, S.K., Guha, A.K., 2009. Jute stick powder as a potential biomass for the removal of congo red and rhodamine B from their aqueous solution. *J. Hazard. Mater.* 164, 374–379.
- Rafatullah, M., Sulaiman, O., Hashim, R., Ahmad, A., 2010. Adsorption of methylene blue on low-cost adsorbents: a review. *J. Hazard. Mater.* 177, 70–80.
- Ramos, M.E., Bonelli, P.R., Blacher, S., Ribeiro Carrott, M.M.L., Carrott, P.J.M., Cukierman, A.L., 2011. Effect of the activating agent on physico-chemical and electrical properties of activated carbon cloths developed from a novel cellulosic precursor. *Colloids Surf. A: Physicochem. Eng. Aspects* 378, 87–93.
- Rodríguez Couto, S., 2009. Dye removal by immobilised fungi. *Biotechnol. Adv.* 27, 227–235.
- Salaices Avila, M.A., Breiter, R., 2008. Competitive sorption of *cis*-DCE and TCE in silica gel as a model porous mineral solid. *Chemosphere* 72, 1807–1815.
- Sud, D., Mahajan, G., Kaur, M.P., 2008. Agricultural waste material as potential adsorbent for sequestering heavy metal ions from aqueous solutions – a review. *Bioresour. Technol.* 99, 6017–6027.
- Tan, I.A.W., Ahmad, A.L., Hameed, B.H., 2008. Adsorption of basic dye using activated carbon prepared from oil palm shell: batch and fixed bed studies. *Desalination* 225, 13–28.
- Vijayaraghavan, K., Yun, Y.S., 2008. Polysulfone-immobilized *Corynebacterium glutamicum*: a biosorbent for reactive black 5 from aqueous solution in an up-flow packed column. *Chem. Eng. J.* 145, 44–49.
- Vilar, V.J.P., Botelho, C.M.S., Boaventura, R.A.R., 2007. Methylene blue adsorption by algal biomass based materials: biosorbents characterization and process behaviour. *J. Hazard. Mater.* 147, 120–132.
- Vilar, V.J.P., Martins, R.J.E., Botelho, C.M.S., Boaventura, R.A.R., 2009. Removal of Cu and Cr from an industrial effluent using a packed-bed column with algae Gelidium-derived material. *Hydrometallurgy* 96, 42–46.
- Yang, Y., Jin, D., Wang, G., Wang, S., Jia, X., Zhao, Y., 2011. Competitive biosorption of acid blue 25 and acid red 337 onto unmodified and CDAB-modified biomass of *Aspergillus oryzae*. *Bioresour. Technol.* 102, 7429–7436.